

Instability of Majorana states in Shiba chains due to leakage into a topological substrate

Nicholas Sedlmayr^{1,*} and Cristina Bena²

¹*Institute of Physics, Maria Curie-Skłodowska University,
Plac Marii Skłodowskiej-Curie 1, PL-20031 Lublin, Poland*

²*Université Paris Saclay, CNRS, CEA, Institut de Physique Théorique, 91191, Gif-sur-Yvette, France*

(Dated: January 25, 2022)

We revisit the problem of Majorana states in chains of scalar impurities deposited on a superconductor with a mixed s-wave and p-wave pairing. We also study the formation of Majorana states for magnetic impurity chains. We find that the magnetic impurity chains exhibit well-localized Majorana states when the substrate is trivial, but these states hybridize and get dissolved in the bulk when the substrate is topological. Most surprisingly, and contrary to previous predictions, the scalar impurity chain does not support fully localized Majorana states except for very small and finely tuned parameter regimes, mostly for a non-topological substrate close to the topological transition. Our results indicate that a purely p-wave or a dominant p-wave substrate are not good candidates to support either magnetic or scalar impurity topological Shiba chains.

I. INTRODUCTION

The presence of impurities in superconductors may give rise under certain conditions to impurity Yu-Shiba-Rusinov states [1–5]. There have been many proposals in the past years to use chains of such bound states to create topological Majorana zero modes (MZMs). [6–43]. One of the most common configurations believed to support Majorana states is a chain of scalar impurities deposited on top of a p-wave superconductor (SC) [44–48].

Recent proposals indicate that the formation of Majorana states is possible even in configurations in which the substrate is a superconductor with mixed s-wave and p-wave components [44, 47]. Such an underlying SC substrate can be in either a topologically trivial or non-trivial phase, depending on the ratio of the s-wave and p-wave components [47]. It has been proposed that a chain of scalar impurities deposited on such a substrate may become topological and exhibit Majorana states for both the regime in which the substrate is topological, as well as for a small region close to the phase transition for which the substrate is topologically trivial [44].

Here we revisit this analysis, as well as we complete it by considering chains of magnetic impurities besides the scalar impurity chains. We perform both tight-binding numerical calculations of the local density of states (LDOS) and Majorana polarization (MP) of the lowest energy states [49–52], as well as calculations of the topological invariant of the chain based on its effective Green's functions [53, 54], and of the quasi-one-dimensional topological invariant [51, 54], the latter two for the magnetic impurity case only. We found that when the substrate itself is topological the Majorana states forming in the chains are not fully localized, they leak in the bulk and hybridize, for both the magnetic and scalar impurity chains. On the other hand, the magnetic

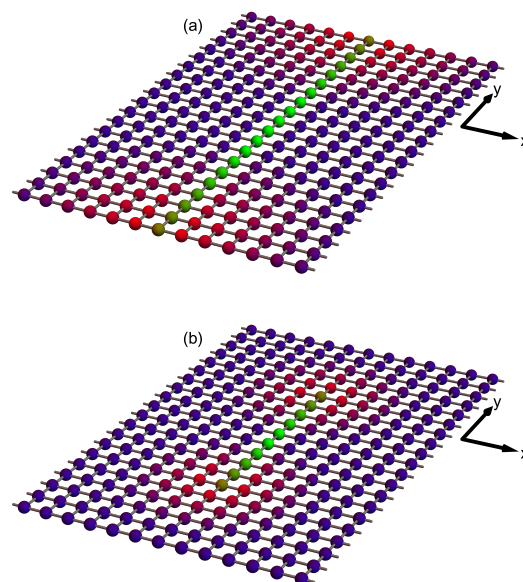


Figure 1. Schematics for the quasi-1D invariant setup (a) versus the numerical TB setup (b). Green sites show the locations of the impurities and a possible localisation of the MZMs is shown in red.

impurity chain may sustain Majorana states for a broad range of parameters, that are fully localized in the wire when the substrate is non-topological and as long as a small p-wave SC component is present. This may occur also for scalar chains but in a much more finely-tuned parameter regime close to the topological transition of the substrate. We analyze also configurations of scalar and magnetic impurity chains on a pure p-wave substrate and we conclude that a pure p-wave SC is not a good candidate to support topological Shiba chains.

The paper is organized as follows: In section II we present the substrate and impurity chain model and the techniques that we will be using. In Section III we present

* e-mail: sedlmayr@umcs.pl

the results for the magnetic and scalar impurity chains. We conclude in Section IV.

II. MODELS AND TECHNIQUES

A. Model

We consider a two dimensional (2D) lattice with a line of embedded impurities. The corresponding momentum-space Hamiltonian for the superconducting substrate in the basis $\psi_{\mathbf{k}} = (c_{\mathbf{k},\uparrow}, c_{\mathbf{k},\downarrow}, c_{-\mathbf{k},\downarrow}^\dagger, -c_{-\mathbf{k},\uparrow}^\dagger)^T$ can be written as:

$$\mathcal{H}_{\mathbf{k}}^{2D} = -[\mu + 2t(\cos k_x + \cos k_y)]\mathbb{I}_2 \otimes \boldsymbol{\tau}^z - \Delta\mathbb{I}_2 \otimes \boldsymbol{\tau}^x + 2\kappa[\sin k_x\boldsymbol{\sigma}^y - \sin k_y\boldsymbol{\sigma}^x] \otimes \boldsymbol{\tau}^x, \quad (1)$$

with μ being the chemical potential, t the nearest-neighbour hopping strength, Δ and κ the s-wave and p-wave superconducting components respectively (both assumed to be real), τ and σ the Pauli matrices in the electron/hole and spin space respectively, and \mathbb{I}_2 a 2×2 identity matrix. The impurities are modeled as on-site potentials $\mathbf{V} = J\boldsymbol{\sigma}^z \otimes \boldsymbol{\tau}^z$ (magnetic impurities) or $\mathbf{V} = U\mathbb{I}_2 \otimes \boldsymbol{\tau}^z$ (scalar impurities), and the real-space Shiba chain Hamiltonian can be written as:

$$\mathcal{H}^{\text{imp}} = \sum_{r \in C} \Psi_r^\dagger \mathbf{V} \Psi_r, \quad (2)$$

with C describing the sites of the one-dimensional chain.

B. Techniques

In order to analyze the topological character of the Shiba impurity chains we will use some standard techniques such as numerical tight-binding as well as techniques that we have introduced in a recent work [54].

1. Effective topological invariant for the Shiba chain

Along the lines of [54] we calculate a topological invariant for the chain based on its 1D effective Green's function \mathcal{G} . Thus, for the Hamiltonian $\mathcal{H}_{\mathbf{k}}^{2D}$ we start with defining the Green's function $\mathcal{G}_0(\omega_n, \mathbf{k}) = (i\omega_n + \mathcal{H}_{\mathbf{k}}^{2D})^{-1}$. The impurity chain is modeled by adding an infinite line described by the potential $\mathbf{V}\delta(x)$. The resulting system can be solved by calculating the T -matrix [55–60]:

$$\mathbf{T} = [\mathbb{I}_4 - \mathbf{V}\mathcal{G}_1(\omega, k_y)]^{-1} \mathbf{V}, \quad (3)$$

where

$$\mathcal{G}_1(\omega, k_y) \equiv \mathcal{G}_1(\omega, x=0, k_y) = \int_{-\pi}^{\pi} \frac{dk_x}{2\pi} \mathcal{G}_0(\omega, \mathbf{k}). \quad (4)$$

The effective Green's function of the Shiba chain ($x=0$) is obtained from the T -matrix formalism:

$$\mathcal{G}(\omega, k_y) = \mathcal{G}_1(\omega, k_y) + \mathcal{G}_1(\omega, k_y) \mathbf{T} \mathcal{G}_1(\omega, k_y). \quad (5)$$

We set $k_y \rightarrow k$ where possible. This Green's function defines an effective Hamiltonian for the chain: $\mathcal{H}_k^{1D} \equiv \mathcal{G}^{-1}(0, k)$.

The model under consideration can have several symmetries important for the topology [61, 62]:

- (i) Particle-hole (PH) symmetry described by an anti-unitary operator $\mathcal{P} = \boldsymbol{\sigma}^y \otimes \boldsymbol{\tau}^y \mathcal{K}$, such that $[\mathcal{P}, \mathcal{H}_k]_+ = 0$ and $\mathcal{P}^2 = 1$. \mathcal{K} is the complex conjugation operator.
- (ii) The “time-reversal” (TR) symmetries described by the anti-unitary operators $\mathcal{T}_+ = i\boldsymbol{\sigma}^z \otimes \boldsymbol{\tau}^0 \mathcal{K}$ and $\mathcal{T}_- = i\boldsymbol{\sigma}^y \otimes \boldsymbol{\tau}^0 \mathcal{K}$, where $[\mathcal{T}_\pm, \mathcal{H}_k]_- = 0$ with $\mathcal{T}_\pm^2 = \pm 1$.
- (iii) Finally we have the combination of PH and TR symmetries, the sublattice or “chiral” symmetry described by the unitary operators $\mathcal{S}_+ = \boldsymbol{\sigma}^x \otimes \boldsymbol{\tau}^y$ and $\mathcal{S}_- = i\boldsymbol{\sigma}^0 \otimes \boldsymbol{\tau}^y$, with $[\mathcal{S}_\pm, \mathcal{H}_k]_- = 0$.

The substrate, in the absence of any impurity potential, has both \mathcal{P} and \mathcal{T}_- symmetries, placing it in the DIII class with Kramer's pairs of topologically protected modes in its topologically non-trivial phases [63]. The \mathcal{T}_+ symmetry is broken by the p-wave term in the x -direction. The addition of scalar impurities does not change the symmetries, however adding magnetic impurities breaks \mathcal{T}_- . The quasi-1D set-up with magnetic impurities therefore possesses only particle-hole symmetry and is in class D with a F_2 invariant. In the strict 1D limit of the chain the \mathcal{T}_- symmetry is recovered, and therefore for the magnetic chain we have both \mathcal{P} and \mathcal{T}_+ symmetries, giving BDI in the classification which has a chiral \mathbb{Z} invariant. For the chain of electronic impurities one must be more careful. In this case we have \mathcal{P} , \mathcal{T}_- , and \mathcal{T}_+ . Therefore one should first diagonalise with respect to the unitary symmetry $\mathcal{U} = \mathcal{T}_- \mathcal{T}_+$. In each diagonalised subblock only a chiral symmetry will remain and the system is in class AIII [63].

For the magnetic impurity chain we can therefore use a standard 1D chiral invariant [54, 64]

$$\nu_{\text{Ch}} = \frac{1}{4\pi i} \int_{-\pi}^{\pi} dk \text{tr} \mathcal{S}_+ \mathcal{H}_k^{1D} \partial_k [\mathcal{H}_k^{1D}]^{-1}. \quad (6)$$

If there are no magnetic impurities then we still have standard time reversal symmetry, and this method no longer captures the appropriate invariant.

2. Numerical tight-binding analysis

We perform a numerical exact diagonalization of the real-space tight-binding model in a periodic-boundary-conditions setup to calculate the wave function corresponding to the lowest-energy state. Choosing periodic

boundary conditions ensures that the edge states associated with the boundaries of the substrate do not interfere with the states localized on the wire. Using the techniques derived in [50] and [51] we calculate the MP associated with the lowest energy states and we plot it as a function of position [50–52, 54]. In most of our analyses we fix the s-wave SC component and we modify the p-wave component. The corresponding topological chain phase diagram is derived by calculating the total MP summed on half the wire [50] as a function of the SC p-wave parameter and the impurity strength (scalar or magnetic). We also calculate the local MP vector and we plot it as a function of position for particular parameter sets. Finally we also use this technique to derive the topological phase diagram in the space of the chemical potential value and impurity strength.

The local MP for a state $|\psi_n\rangle$ is defined as

$$M_{\mathbf{r}} = e^{i\varphi} \langle \psi_n | \hat{\mathbf{r}} \mathcal{P} | \psi_n \rangle, \quad (7)$$

where $\hat{\mathbf{r}} \mathcal{P}$ is the spatial projection of the particle-hole operator \mathcal{P} . The overall phase φ is arbitrary. The total MP is therefore

$$M = \left| \sum_{\mathbf{r} \in C'} M_{\mathbf{r}} \right|, \quad (8)$$

with C' being the set of all the sites in the left half of the impurity chain. For a well defined MZM one has

$$M = \rho' \equiv \sum_{\mathbf{r} \in C'} \rho_{\mathbf{r}}, \quad (9)$$

with

$$\rho_{\mathbf{r}} = \langle \psi_n | \hat{\mathbf{r}} | \psi_n \rangle \quad (10)$$

denoting the LDOS distribution corresponding to the state $|\psi_n\rangle$.

When time reversal symmetry is present, see section II B 1, we must also be careful with the states that we consider in the degenerate subspace. In this case the MZMs always come in degenerate Kramer's pairs, with one pair localized at one end of the chain. If we consider two such degenerate MZMs $|\psi_{01}\rangle$ and $|\psi_{02}\rangle$, it is clear that an arbitrary combination of the two is no longer an eigenstate of the particle-hole operator. For example, if $\mathcal{P}|\psi_{01,2}\rangle = |\psi_{01,2}\rangle$ then

$$\begin{aligned} \mathcal{P} [a e^{i\alpha} |\psi_{01}\rangle + b e^{i\beta} |\psi_{02}\rangle] &= a e^{-i\alpha} |\psi_{01}\rangle + b e^{-i\beta} |\psi_{02}\rangle \\ &\neq e^{i\gamma} [a e^{i\alpha} |\psi_{01}\rangle + b e^{i\beta} |\psi_{02}\rangle], \end{aligned} \quad (11)$$

where a, b, α, β , and γ are real with $a^2 + b^2 = 1$. For the numerical calculation of the MP it is therefore always important to rotate within the degenerate subspace to a basis of two MZMs.

3. Invariant from Quasi-1D Strip

An alternative route to calculating the invariant is to treat the impurity chain plus substrate as a quasi-1D system, consisting of one line of impurity sites and on either side a number of lines of sites of the background 2D lattice, totalling N_x lines [51, 54]. We then calculate the invariant for different N_x . In the limit that N_x is large the invariant should no longer depend explicitly on N_x . The invariant is given by the parity of the negative energy bands at the time reversal invariant momenta [65]. Following an appropriate rotation the Hamiltonian can be written at the time reversal invariant momenta as $H_{0,\pi}^{\text{Q1D}} \rightarrow \text{diag}(\bar{\mathcal{H}}(0, \pi), -\bar{\mathcal{H}}(0, \pi))$, and calculating the parity of the negative energy bands is then equivalent to calculating

$$\delta = (-1)^{\nu_{\text{Q1D}}} = \text{sgn} [\det \bar{\mathcal{H}}(0) \det \bar{\mathcal{H}}(\pi)]. \quad (12)$$

Note that this system does not have chiral symmetry, so it is in the D class which has a \mathbb{Z}_2 invariant, and hence we can write

$$\nu_{\text{Q1D}} = \frac{1 - \text{sgn} [\det \bar{\mathcal{H}}(0) \det \bar{\mathcal{H}}(\pi)]}{2}. \quad (13)$$

We should note that the result of this calculation is not exactly what we are looking for in the present configuration: the quasi-1D topological invariant predicts the formation of chain end states for a setup in which the impurity chain ends exactly at the same position as the strip (see Fig. 1). This does not capture the same physics as that of a chain fully embedded in an infinite substrate, thus the results obtained using this method are only indicative of the underlying physics, but do not capture for example accurately the destruction of the Majorana modes in the chain via a leakage in the substrate. We will thus use them as a basis and comparison for the rest of the results. Also note once more that this technique only works for magnetic impurities and not for scalar ones.

III. RESULTS

A. Magnetic impurities

In Fig. 2 we plot the energy and the MP of the lowest energy state, as well as the GF invariants as a function of the p-wave SC component and the magnetic impurity strength. The s-wave SC component is fixed at $\Delta = 0.16$, same as in Ref. 44.

Note that the quasi-1D invariant predicts a wide range of parameters for which the system is topological. As described in Fig. 1 this corresponds to cutting the entire system in half and recovering end states when the end of the chain corresponds exactly to the end of the wire. However, this is not what happens in more realistic setups, thus the phase diagram obtained by calculating the MP in the wire is more relevant for an experimental

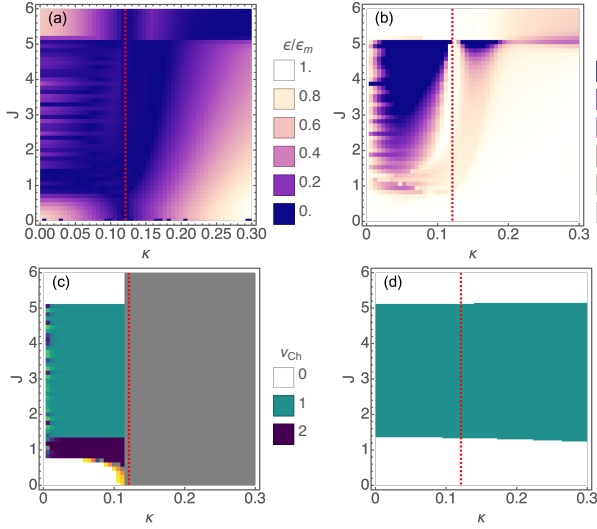


Figure 2. A comparison of the lowest energy state energy (a), MP (b), GF invariant (c) and quasi-1D invariant (d) for a chain of magnetic impurities within a 2D *s*-wave/*p*-wave lattice, as a function of the *p*-wave parameter κ and the magnetic impurity strength J . Here $\Delta = 0.16t$ and $\mu = 3.5$. The system size is 21×80 with a gap of 20 sites between the boundary of the system and the end of the chain, periodic boundary conditions are imposed. The red dashed line is the substrate topological phase boundary $\kappa > \Delta\sqrt{2}/\mu$. The grey region in (c), which matches the region where the substrate is topologically non-trivial, is where the integral for the invariant did not converge in time. The maximum energy in the phase diagram ($\epsilon_m = 0.225t$) is used to scale the energy plot.

situation corresponding to that in Fig. 1b). The corresponding phase diagram indicates that the Majorana states forming in the wire leak significantly in the bulk if the substrate is topologically non-trivial (for $\kappa > \Delta\sqrt{2}/\mu$ and $\mu < 4t$). In this regime only a part of the weight of the lowest-energy states is localized in the wire, while the rest is distributed in the bulk, either in the vicinity of the end, or parallel to the wire itself. Such configurations are shown in Figs. 3 (a) and (b). We note that, moreover, the local MP vectors in this situation are not aligned inside a certain region (that would be consistent to the formation of a proper Majorana state), but precess, indicating that the corresponding states are not actual Majorana, but quasi-Majorana, even if their energy is very close to zero. They thus cannot be fully separated and could not be properly used as qubits.

When the substrate is topologically trivial (for $\kappa < \Delta\sqrt{2}/\mu$) the lowest-energy states actually become fully localized in the chain and the MP is getting close to 1, indicating very small leaks in the bulk. In Fig. 4 we show the density and local Majorana polarisation in such a situation.

Note that when the substrate is trivial, the results for the topological character of the wire obtained by calculating the GF invariant (Fig. 2c) are similar to those obtained by the MP calculation (Fig. 2b) and the quasi-1D

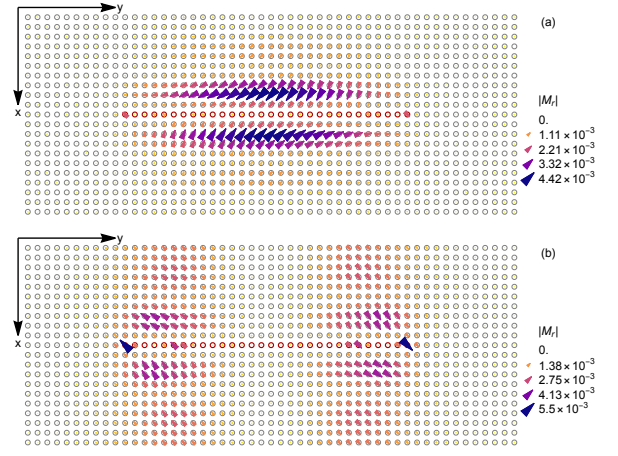


Figure 3. The MP for two points in the phase space for which the substrate is topological. We take $\Delta = 0.16t$ and $\mu = 3.5t$. For panel (a) $J = 3t$, $\kappa = 0.2t$, and for panel (b) $J = 1.8t$, $\kappa = 0.14t$. Note that the MP vector precesses and that the LDOS of the lowest energy states leaks into the bulk either parallel to the wire or close to the ends, see panels (a) and (b) respectively). The system size is 21×70 with a gap of 20 sites between the boundary of the system and the end of the chain, periodic boundary conditions are imposed.

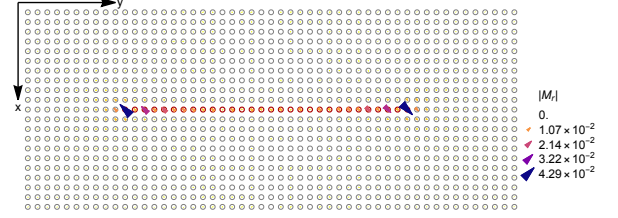


Figure 4. The LDOS and MP for a point in the phase space for which the substrate is non-topological. We take $J = 3t$, $\Delta = 0.16t$, $\mu = 3.5t$, and $\kappa = 0.05t$. Note that the MP vector and the LDOS of the lowest energy states are concentrated mainly on the chain. The system size is 61×70 with a gap of 20 sites between the boundary of the system and the end of the chain, periodic boundary conditions are imposed.

invariant (Fig. 2d). However, when the substrate is topologically non-trivial the integral for the GF invariant in Eq. (6) converges very slowly: due to the complex form of the integrand the integral over k is implemented as a simple Riemann sum with a number of steps $N_{\text{Ch}} = 200$. For the topologically non-trivial substrate this integral does not converge with N_{Ch} , and a scaling analysis shows that not only will it not converge except for numerically unattainable N_{Ch} , but also that in the limit of $N_{\text{Ch}} \rightarrow \infty$ we will have $\nu_{\text{Ch}} \rightarrow 1$ irrespective of whether the wire itself is topological or not, indicating that in this particular case the invariant tracks rather the topological character of the 2D substrate.

We note that the physics of a magnetic impurity chain on a trivial substrate with a non-zero *p*-wave component is very similar to that for an *s*-wave SC substrate with

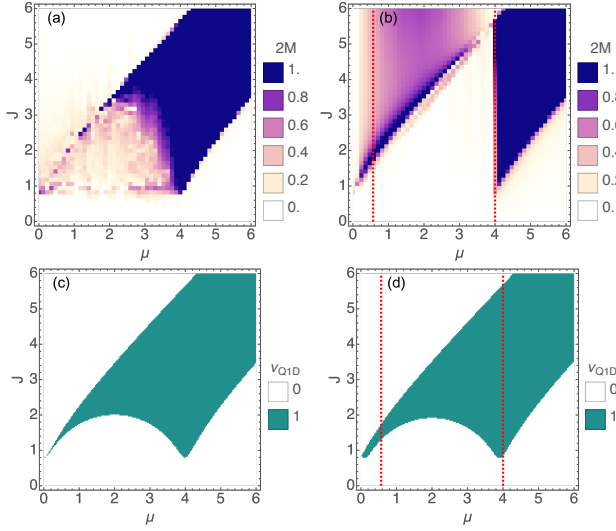


Figure 5. The MP and the quasi 1D invariant as a function of μ and J . Here $\Delta = 0.16t$, with $\kappa = 0.05t$ (on the left) and $\kappa = 0.3t$ (on the right). The system size is 21×80 with a gap of 20 sites between the boundary of the system and the end of the chain, and we impose periodic boundary conditions. The red dashed lines indicate the topological phase boundary for the substrate $2\Delta^2/\kappa^2 < \mu < 4t$. For (a,c) there is no non-trivial phase in the substrate as $2\Delta^2/\kappa^2 > 4t$.

Rashba spin-orbit coupling. It appears that the p-wave component of the SC, no matter how small, would play the role of the spin-orbit coupling, and thus Majorana states would form also for a chain of magnetic impurities deposited on a substrate with a small but non-zero p-wave component. To check this we consider a combination of an s-wave component $\Delta = 0.16t$ and a p-wave one $\kappa = 0.05t$, and we plot the MP as a function of μ and J (see Fig. 5 top left panel). Indeed we recover exactly the same profile as in the topological phase diagram as function of μ and J in the presence of spin-orbit coupling in the substrate [54]. This makes us believe that the Rashba spin-orbit coupling is equivalent to a small p-wave component in what concerns the formation of Majorana states in chains of magnetic impurities. We note that for a larger p-wave component, $\kappa = 0.3t > \Delta\sqrt{2/\mu}$ (see Fig. 5 top right panel) the corresponding (μ, J) topological phase diagram indicates that the wire becomes topological only when the substrate is not (e.g. $\mu > 4t$).

To conclude this section we consider the case of a pure p-wave, and in Fig. 6 we plot the MP as a function of position for a chain of magnetic impurities. We note that the lowest-energy states in the wire leak strongly in the substrate, consistent with what we observed also for the mixed s+p SC substrate with a dominant p-wave component. Thus we claim that clean and isolated Majorana states cannot be obtained on a topological substrate by depositing magnetic impurities, but they can be obtained when the substrate is non-topological with either a Rashba or a small p-wave component.

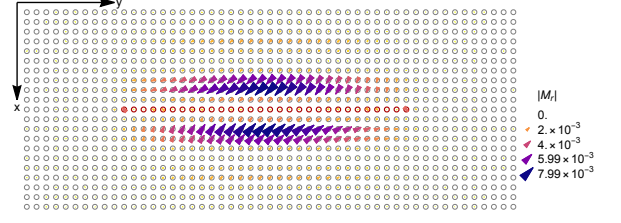


Figure 6. The LDOS and MP for a chain of magnetic impurities on a pure p-wave substrate. We take $J = 3t$, $\Delta = 0t$, $\mu = 3.5t$, and $\kappa = 0.2t$. The system size is 21×70 with a gap of 20 sites between the boundary of the system and the end of the chain, periodic boundary conditions are imposed.

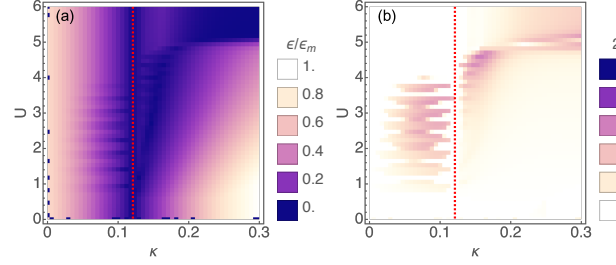


Figure 7. A comparison of the lowest energy state energy and the MP for a chain of scalar impurities deposited on a 2D s-wave/p-wave lattice, as a function of the p-wave parameter κ and the scalar impurity strength U . Here $\Delta = 0.16t$ and $\mu = 3.5$. The system size is 21×80 with a gap of 20 sites between the end of the chain and the system boundary, and periodic boundary conditions are imposed. The red dashed lines indicate the topological phase boundary for the substrate $\kappa > \Delta\sqrt{2/\mu}$. The maximum energy in the phase diagram ($\epsilon_m = 0.225t$) is used to scale the energy plot.

B. Scalar impurities

In this configuration the time reversal symmetry is preserved. It is difficult to calculate an appropriate TRS invariant from an effective Green's function, as well as a quasi-1D invariant. Thus we base our analysis on numerical tight-binding and we calculate the topological phase diagrams based on the MP of the lowest-energy states. In Fig. 7 we plot the MP of the lowest-energy state as a function of the p-wave SC component and the value of the impurity potential U , for a fixed value of the s-wave SC component $\Delta = 0.16t$.

The topological transition between a topological and trivial bulk would take place around $\kappa = \Delta\sqrt{2/\mu}$. For larger p-wave pairings the substrate is topological, and for smaller ones it is trivial. From Fig. 7 we can see that the MP is significant on the wire only for a very finely tuned region, mostly localized around the bulk topological transition, for a region in which the substrate is non-topological. Moreover, for the system sizes considered, the MP values obtained are not perfect as observed for the magnetic impurity chains ($2M \approx 1$), indicating a fragility for these states, whose perfect Majorana char-

acter cannot even be fully recovered numerically here. The formation of Majorana states in the presence of a scalar impurity chain on a non-topological substrate was predicted in [44], as well as in [47]. Indeed we recover here the same phenomenon, however, we note that the existence of fully localized and distinct Majorana states is only possible when the substrate is trivial, in a very finely-tuned region, for the rest of the parameter phase space the Majoranas leak in the bulk and they cannot be considered isolated states that would allow for example their use as qubits.

In Fig. 8 we show plots of the density and local Majorana polarisation. When the substrate is topological the impurity states leak into the substrate and hybridise with the bulk states, see Fig. 8(a) and (b). The spatial profiles are similar to those obtained for magnetic impurities. When we place our parameters in the finely tuned region close to the topological bulk transition we observe better localized and polarized Majorana states, see Fig. 8(c). When the substrate is trivial, far from the topological transition, the states arising on the wire have negligible Majorana polarization, see Fig. 8(d).

We also plot the MP phase diagram as a function of the chemical potential μ and the scalar impurity potential U (see Fig. 9) for an s-wave component $\Delta = 0.16t$ and two values of the p-wave parameter putting the substrate for $\mu < 4t$ in the topological phase ($\kappa = 0.3t$), as well as in the non-topological phase close to the transition ($\kappa = 0.1t$). We note that, same as for the magnetic impurity case, for a large value of $\kappa > \Delta\sqrt{2/\mu}$ the the chain becomes topological only when the when the substrate is not (e.g. $\mu > 4t$), however when κ is slightly smaller than $\Delta\sqrt{2/\mu}$ we recover a slightly more extended topological phase diagram.

Same as for the magnetic impurity we also consider the case of a pure p-wave, and in Fig. 10 we plot the MP as a function of position for a chain of scalar impurities. We note that the lowest-energy states in the wire also leak strongly in the substrate. Thus we conclude that clean and isolated Majorana states cannot be obtained on a topological substrate by depositing scalar impurities on a p-wave substrate, and we confirm our previous observation that it is quasi-impossible to recover clean Majorana states in a chain of impurities deposited on a topological substrate.

IV. CONCLUSION

We have revisited the problem of chains of scalar impurities deposited on an SC substrate with mixed p-wave and s-wave components. We have also explored a similar configuration involving magnetic-impurity chains. We have found that when the substrate itself is topological the Majorana states forming in the chains are not fully localized, they leak in the bulk and hybridize, thus not making good quantum qubit candidates. On the other hand when the substrate is trivial the magnetic impurity

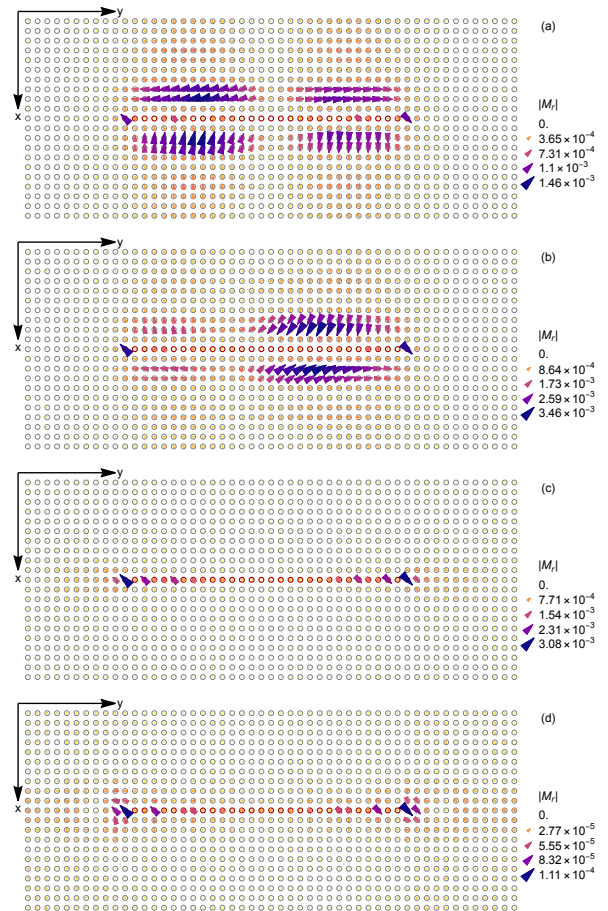


Figure 8. The LDOS and MP for a point in the phase space for which the substrate is topological (a) $U = 2t$, $\kappa = 0.2t$ and b) $U = 3t$, $\kappa = 0.2t$), non-topological close to the phase transition (c) $U = 2t$, $\kappa = 0.1t$) and far from it (d) $U = 1t$, $\kappa = 0.02t$). We take $\Delta = 0.16t$ and $\mu = 3.5t$. Note that the MP vector and the LDOS of the lowest energy states are leaking in the bulk for a) and b), are concentrated mainly on the chain for c), and there is negligible Majorana character for d). The system size is 21×70 (a,b) or 61×70 (c,d), with a gap of 20 sites between the boundary of the system and the end of the chain, periodic boundary conditions are imposed.

chains can sustain clean Majorana states, well localized on the wire. This may happen also for scalar chains but in a much more finely-tuned parameter regime and with a much more difficulty to obtain localization. A pure p-wave substrate would thus not be a good candidate to support topological Shiba chains, however a small p-wave component would make this possible for a chain of magnetic impurities.

ACKNOWLEDGMENTS

This work was supported by the National Science Centre (NCN, Poland) under the grant 2019/35/B/ST3/03625 (NS). We would like to thank

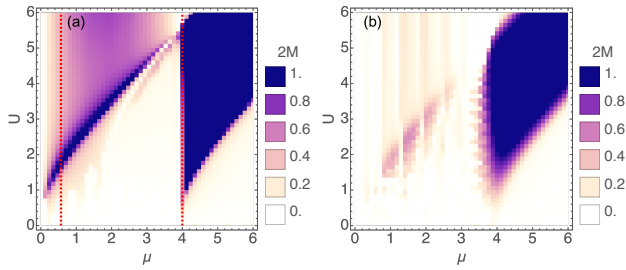


Figure 9. The MP as a function of μ and U in the bulk topological phase $\kappa = 0.3t$ (a) and bulk non-topological phase close to the phase transition $\kappa = 0.1t$ (b). The system size is 21×80 with a gap of 20 sites between the impurities and the system end and periodic boundary conditions. The red dashed lines indicate the topological phase boundary for the substrate $2\Delta^2/\kappa^2 < \mu < 4t$. For (b) there is no non-trivial phase in the substrate as $2\Delta^2\kappa^2 > 4t$.

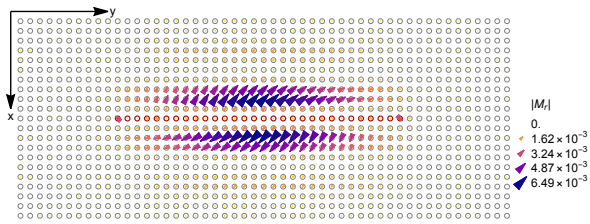


Figure 10. The MP for a point in the phase space for a pure p-wave substrate. We take $U = 3t$, $\Delta = 0t$, $\mu = 3.5t$, and $\kappa = 0.2t$. The system size is 21×70 with a gap of 20 sites between the boundary of the system and the end of the chain, periodic boundary conditions are imposed.

Vardan Kaladzhyan for interesting discussions.

Appendix A: Energy Scaling and Boundary Conditions

In this appendix we demonstrate that there is a fundamental difference between open boundary conditions and periodic boundary conditions for the zero modes. In Fig. 11 we show the energy scaling of the lowest eigenvalues for a system with periodic and open boundary conditions in a regime which has a non-trivial quasi 1D invariant. As expected this system has an exponentially small eigenvalue. However for periodic boundary conditions in the lateral direction there is no zero mode.

Appendix B: Additional phase diagrams

Here we present additional phase diagrams calculated using the chiral invariant, see Fig. 12, to be compared to Fig. 5. As before, when the substrate is topologically non-trivial the numerical integral over k does not converge with the used number of steps in the Riemann sum.

- [1] LUH Yu, “Bound State in Superconductors With Paramagnetic Impurities,” *Acta Physica Sinica* **21**, 75–91 (1965).
- [2] Hiroyuki Shiba, “Classical Spins in Superconductors,” *Progress of Theoretical Physics* **40**, 435–451 (1968).
- [3] A. I. Rusinov, “Superconductivity near a Paramagnetic Impurity,” *JETP Letters* **9**, 85–85 (1969).
- [4] Ali Yazdani, B. A. Jones, C. P. Lutz, M. F. Crommie, and D. M. Eigler, “Probing the local effects of magnetic impurities on superconductivity,” *Science* **275**, 1767–1770 (1997).
- [5] Gerbold C. Ménard, Sébastien Guissart, Christophe Brun, Stéphane Pons, Vasily S. Stolyarov, François Debontridder, Matthieu V. Leclerc, Etienne Janod, Laurent Cario, Dimitri Roditchev, Pascal Simon, and Tristan Cren, “Coherent long-range magnetic bound states in a superconductor,” *Nature Physics* **11**, 1013–1016 (2015).
- [6] S. Nadj-Perge, I. K. Drozdov, B. A. Bernevig, and Ali Yazdani, “Proposal for realizing Majorana fermions in chains of magnetic atoms on a superconductor,” *Physical Review B* **88**, 20407–20407 (2013).
- [7] Falko Pientka, Leonid I. Glazman, and Felix Von Oppen, “Topological superconducting phase in helical Shiba chains,” *Physical Review B* **88**, 155420–155420 (2013).

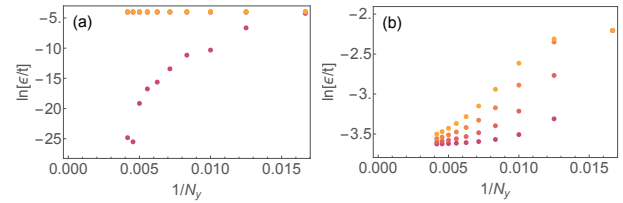


Figure 11. Lowest energies of the system with magnetic impurities as a function of inverse system length N_y^{-1} for (a) open boundary conditions and (b) periodic boundary conditions along x . This is for $N_x = 21$, $J = 3t$, $U = 0$, $\Delta = 0.16t$, $\mu = 3.5t$, and $\kappa = 0.2$, when the substrate is topologically non-trivial and ν_{Q1D} is also non-trivial.

- [8] Bernd Braunecker and Pascal Simon, “Interplay between classical magnetic moments and superconductivity in quantum one-dimensional conductors: Toward a self-sustained topological majorana phase,” *Physical Review Letters* **111**, 147202–147202 (2013).
- [9] Jelena Klinovaja and Daniel Loss, “Giant spin-orbit interaction due to rotating magnetic fields in graphene nanoribbons,” *Physical Review X* **3**, 1–6 (2013).

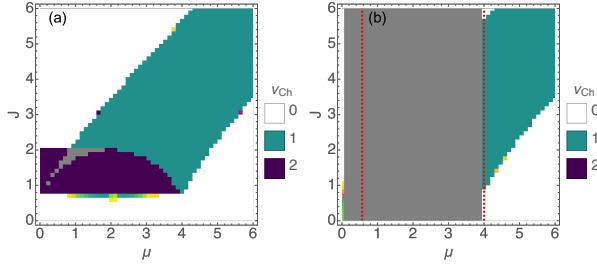


Figure 12. The chiral invariant as a function of μ and J , to compare with Fig. 5. Here $\Delta = 0.16t$ with $\kappa = 0.05t$ (a) and $\kappa = 0.3t$ (b). The red dashed lines indicate the topological phase boundary for the substrate $2\Delta^2/\kappa^2 < \mu < 4t$. For (a) there is no non-trivial phase in the substrate as $2\Delta^2\kappa^2 > 4t$. The grey region indicates the points where the integral for the chiral invariant did not converge in the available time.

- [10] M. M. Vazifeh and M. Franz, “Self-organized topological state with majorana fermions,” *Physical Review Letters* **111**, 206802–206802 (2013).
- [11] Falko Pientka, Leonid I. Glazman, and Felix von Oppen, “Unconventional topological phase transitions in helical Shiba chains,” *Physical Review B* **89**, 180505 (2014).
- [12] Kim Pöyhönen, Alex Westström, Joel Röntynen, and Teemu Ojanen, “Majorana states in helical Shiba chains and ladders,” *Physical Review B* **89**, 115109–115109 (2014).
- [13] I. Reis, D. J. J. Marchand, and M. Franz, “Self-organized topological state in a magnetic chain on the surface of a superconductor,” *Physical Review B* **90**, 085124 (2014).
- [14] E. H. Kim, “Characterizing topological order in superconductors via entanglement,” *Journal of Physics: Condensed Matter* **26**, 205602–205602 (2014).
- [15] Jian Li, Hua Chen, Ilya K. Drozdov, A. Yazdani, B. Andrei Bernevig, and A. H. MacDonald, “Topological superconductivity induced by ferromagnetic metal chains,” *Physical Review B* **90**, 235433 (2014).
- [16] Andreas Heimes, Panagiotis Kotetes, and Gerd Schön, “Majorana fermions from Shiba states in an antiferromagnetic chain on top of a superconductor,” *Physical Review B* **90**, 60507–60507 (2014).
- [17] P. M. R. Brydon, S. Das Sarma, Hoi-Yin Hui, and Jay D. Sau, “Topological Yu-Shiba-Rusinov chain from spin-orbit coupling,” *Physical Review B* **91**, 064505 (2015).
- [18] Alex Westström, Kim Pöyhönen, and Teemu Ojanen, “Topological properties of helical Shiba chains with general impurity strength and hybridization,” *Physical Review B* **91**, 064502 (2015).
- [19] Andreas Heimes, Daniel Mendler, and Panagiotis Kotetes, “Interplay of topological phases in magnetic adatom-chains on top of a Rashba superconducting surface,” *New Journal of Physics* **17**, 23051–23051 (2015).
- [20] Yang Peng, Falko Pientka, Leonid I. Glazman, and Felix Von Oppen, “Strong localization of majorana end states in chains of magnetic adatoms,” *Physical Review Letters* **114**, 106801–106801 (2015).
- [21] Hoi-Yin Hui, P. M. R. Brydon, Jay D. Sau, S. Tewari, and S. Das Sarma, “Majorana fermions in ferromagnetic chains on the surface of bulk spin-orbit coupled s-wave superconductors,” *Scientific Reports* **5**, 8880 (2015).
- [22] Joel Röntynen and Teemu Ojanen, “Topological Superconductivity and High Chern Numbers in 2D Ferromagnetic Shiba Lattices,” *Physical Review Letters* **114**, 236803 (2015).
- [23] Bernd Braunecker and Pascal Simon, “Self-stabilizing temperature-driven crossover between topological and nontopological ordered phases in one-dimensional conductors,” *Physical Review B* **92**, 241410 (2015).
- [24] Kim Pöyhönen, Alex Westström, and Teemu Ojanen, “Topological superconductivity in ferromagnetic atom chains beyond the deep-impurity regime,” *Physical Review B* **93**, 014517 (2016).
- [25] Xichao Zhang, Yan Zhou, and Motohiko Ezawa, “Antiferromagnetic Skyrmion: Stability, Creation and Manipulation,” *Scientific Reports* **6**, 1–8 (2016).
- [26] Wan Ju Li, Sung Po Chao, and Ting Kuo Lee, “Theoretical study of large proximity-induced s -wave-like pairing from a d -wave superconductor,” *Physical Review B* **93**, 35140–35140 (2016).
- [27] Joel Röntynen and Teemu Ojanen, “Chern mosaic: Topology of chiral superconductivity on ferromagnetic adatom lattices,” *Physical Review B* **93**, 94521–94521 (2016).
- [28] Silas Hoffman, Jelena Klinovaja, and Daniel Loss, “Topological phases of inhomogeneous superconductivity,” *Physical Review B* **93**, 165418 (2016).
- [29] Jian Li, Titus Neupert, Zhijun Wang, A. H. MacDonald, A. Yazdani, and B. Andrei Bernevig, “Two-dimensional chiral topological superconductivity in Shiba lattices,” *Nature Communications* **7**, 12297 (2016).
- [30] Michael Schecter, Karsten Flensberg, Morten H Christensen, Brian M Andersen, and Jens Paaske, “Self-organized topological superconductivity in a Yu-Shiba-Rusinov chain,” *Physical Review B* **93**, 140503 (2016).
- [31] Morten H Christensen, Michael Schecter, Karsten Flensberg, Brian M Andersen, and Jens Paaske, “Spiral magnetic order and topological superconductivity in a chain of magnetic adatoms on a two-dimensional superconductor,” *Physical Review B* **94**, 144509 (2016).
- [32] Vardan Kaladzhyan, Julien Despres, Ipsita Mandal, and Cristina Bena, “Majorana fermions in finite-size strips with in-plane magnetic fields,” *European Physical Journal B* **90** (2017), 10.1140/epjb/e2017-80103-y.
- [33] Gian Marcello Andolina and Pascal Simon, “Topological properties of chains of magnetic impurities on a superconducting substrate: Interplay between the Shiba band and ferromagnetic wire limits,” *Physical Review B* **96**, 235411 (2017).
- [34] Aksel Kobjalka, Nicholas Sedlmayr, Maciej M. Maška, and Tadeusz Domański, “Dimerization-induced topological superconductivity in a Rashba nanowire,” *Physical Review B* **101**, 085402 (2020).
- [35] Gerbold C. Ménard, Sébastien Guissart, Christophe Brun, Raphaël T. Leriche, Mircea Trif, François Debontridder, Dominique Demaille, Dimitri Roditchev, Pascal Simon, and Tristan Cren, “Two-dimensional topological superconductivity in Pb/Co/Si(111),” *Nature Communications* **8**, 2040 (2017).
- [36] Gerbold C. Ménard, Andrej Mesaros, Christophe Brun, François Debontridder, Dimitri Roditchev, Pascal Simon, and Tristan Cren, “Isolated pairs of Majorana zero modes in a disordered superconducting lead monolayer,” *Nature Communications* **10**, 2587 (2019).

- [37] Stevan Nadj-Perge, Ilya K. Drozdov, Jian Li, Hua Chen, Sangjun Jeon, Jungpil Seo, Allan H. MacDonald, B. Andrei Bernevig, and Ali Yazdani, “Observation of Majorana fermions in ferromagnetic atomic chains on a superconductor,” *Science* **346**, 602–607 (2014).
- [38] Remy Pawlak, Marcin Kisiel, Jelena Klinovaja, Tobias Meier, Shigeki Kawai, Thilo Glatzel, Daniel Loss, and Ernst Meyer, “Probing Atomic Structure and Majorana Wavefunctions in Mono-Atomic Fe-chains on Superconducting Pb-Surface,” *npj Quantum Information* **2**, 16035–16035 (2015).
- [39] Michael Ruby, Falko Pientka, Yang Peng, Felix von Oppen, Benjamin W. Heinrich, and Katharina J. Franke, “End States and Subgap Structure in Proximity-Coupled Chains of Magnetic Adatoms,” *Physical Review Letters* **115**, 197204 (2015).
- [40] Benjamin E. Feldman, Mallika T. Randeria, Jian Li, Sangjun Jeon, Yonglong Xie, Zhijun Wang, Ilya K. Drozdov, B. Andrei Bernevig, and Ali Yazdani, “High-resolution studies of the Majorana atomic chain platform,” *Nature Physics* **13**, 286–291 (2017).
- [41] Michael Ruby, Benjamin W. Heinrich, Yang Peng, Felix von Oppen, and Katharina J. Franke, “Exploring a Proximity-Coupled Co Chain on Pb(110) as a Possible Majorana Platform,” *Nano Letters* **17**, 4473–4477 (2017).
- [42] Se Kwon Kim, Roberto Myers, and Yaroslav Tserkovnyak, “Nonlocal Spin Transport Mediated by a Vortex Liquid in Superconductors,” *Physical Review Letters* **121**, 187203–187203 (2018).
- [43] Rémy Pawlak, Silas Hoffman, Jelena Klinovaja, Daniel Loss, and Ernst Meyer, “Majorana fermions in magnetic chains,” *Progress in Particle and Nuclear Physics* **107**, 1–19 (2019).
- [44] Titus Neupert, A. Yazdani, and B. Andrei Bernevig, “Shiba chains of scalar impurities on unconventional superconductors,” *Physical Review B* **93**, 094508 (2016).
- [45] Isac Sahlberg, Alex Westström, Kim Pöyhönen, and Teemu Ojanen, “Engineering one-dimensional topological phases on p-wave superconductors,” *Physical Review B* **95**, 184512 (2017).
- [46] Vardan Kaladzhyan, Joel Röntynen, Pascal Simon, and Teemu Ojanen, “Topological state engineering by potential impurities on chiral superconductors,” *Physical Review B* **94**, 60505–60505 (2016).
- [47] V. Kaladzhyan, Cristina Bena, and Pascal Simon, “Topology from triviality,” *Physical Review B* **97**, 104512 (2018).
- [48] Andreas Kreisel, Timo Hyart, and Bernd Rosenow, “Tunable topological states hosted by unconventional superconductors with adatoms,” *Physical Review Research* **3**, 033049 (2021), arXiv:2102.12502.
- [49] Doru Sticlet, Cristina Bena, and Pascal Simon, “Spin and majorana polarization in topological superconducting wires,” *Physical Review Letters* **108**, 96802–96802 (2012).
- [50] N. Sedlmayr and C. Bena, “Visualizing Majorana bound states in one and two dimensions using the generalized Majorana polarization,” *Physical Review B* **92**, 115115–115115 (2015).
- [51] N. Sedlmayr, J. M. Aguiar-Hualde, and C. Bena, “Majorana bound states in open quasi-one-dimensional and two-dimensional systems with transverse Rashba coupling,” *Physical Review B* **93**, 155425–155425 (2016).
- [52] Szczepan Głodzik, Nicholas Sedlmayr, and Tadeusz Domański, “How to measure the Majorana polarization of a topological planar Josephson junction,” *Physical Review B* **102**, 085411 (2020).
- [53] Sarah Pinon, Vardan Kaladzhyan, and Cristina Bena, “Surface Green’s functions and boundary modes using impurities: Weyl semimetals and topological insulators,” *Physical Review B* **101**, 115405 (2020).
- [54] Nicholas Sedlmayr, Vardan Kaladzhyan, and Cristina Bena, “Analytical and semianalytical tools to determine the topological character of Shiba chains,” *Physical Review B* **104**, 024508 (2021), arXiv:2102.02214.
- [55] J. M. Byers, M. E. Flatté, and D. J. Scalapino, “Influence of gap extrema on the tunneling conductance near an impurity in an anisotropic superconductor,” *Physical Review Letters* **71**, 3363–3366 (1993).
- [56] M. I. Salkola, A. V. Balatsky, and D. J. Scalapino, “Theory of Scanning Tunneling Microscopy Probe of Impurity States in a D-Wave Superconductor,” *Physical Review Letters* **77**, 1841–1844 (1996).
- [57] W. Ziegler, D. Poilblanc, R. Preuss, W. Hanke, and D. J. Scalapino, “ T -matrix formulation of impurity scattering in correlated systems,” *Physical Review B* **53**, 8704–8707 (1996).
- [58] Gerald D. Mahan, *Many-Particle Physics* (Springer US, Boston, MA, 2000).
- [59] A. V. Balatsky, I. Vekhter, and Jian-Xin Zhu, “Impurity-induced states in conventional and unconventional superconductors,” *Reviews of Modern Physics* **78**, 373–433 (2006).
- [60] Cristina Bena, “Friedel oscillations: Decoding the hidden physics,” *Comptes Rendus Physique* **17**, 302–321 (2016).
- [61] Ching Kai Chiu, Jeffrey C.Y. Teo, Andreas P. Schnyder, and Shinsei Ryu, “Classification of topological quantum matter with symmetries,” *Reviews of Modern Physics* **88**, 035005 (2016).
- [62] Masatoshi Sato and Yoichi Ando, “Topological superconductors : A review,” *Reports on Progress in Physics* , aa6ac7–aa6ac7 (2017).
- [63] Shinsei Ryu, Andreas P. Schnyder, Akira Furusaki, and Andreas W W Ludwig, “Topological insulators and superconductors: Tenfold way and dimensional hierarchy,” *New Journal of Physics* **12**, 65010–65010 (2010).
- [64] V. Gurarie, “Single-particle Green’s functions and interacting topological insulators,” *Physical Review B* **83**, 085426 (2011).
- [65] Masatoshi Sato, “Topological properties of spin-triplet superconductors and Fermi surface topology in the normal state,” *Physical Review B* **79**, 214526–214526 (2009).